# EBG Based Microstrip Patch antenna for Brain Tumor Detection via Scattering Parameters in Microwave Imaging System

Reefat Inum, *Student Member, IEEE*, Md. Masud Rana, *Member, IEEE*, and Kamrun Nahar Shushama, *Student Member, IEEE*

Department of Electrical and Electronic Engineering

Rajshahi University of Engineering and Technology

Email: romel.eee09@gmail.com, md.masud.rana@ruet.ac.bd, shushamanahar@gmail.com

**Abstract**

A microwave brain imaging system model is envisaged to detect and visualize tumor inside the human brain. A compact and efficient microstrip patch antenna is used in the imaging technique to transmit equivalent signal and receive backscattering signal from the stratified human head model. Electromagnetic band gap (EBG) structure is incorporated on the antenna ground plane to enhance the performance. Rectangular and circular EBG structures are proposed to investigate the antenna performance. Incorporation of circular EBG on the antenna ground plane provides an improvement of 22.77% in return loss, 5.84% in bandwidth, and 13.23% in antenna gain with respect to the patch antenna with rectangular EBG. Specific absorption rate (SAR) of the modeled head tissue for the proposed antenna is determined. Different SAR values are compared with the established standard SAR limit to provide a safety regulation of the imaging system. A confocal microwave imaging algorithm is applied to generate the image of tumor inside a six layer human head phantom model. S-parameter signals obtained from circular EBG loaded patch antenna in different scanning modes are utilized in the imaging algorithm to effectively produce a high resolution image which reliably indicates the presence of tumor inside human brain.

**keywords:** EBG, Microstrip patch antenna, Microwave imaging, Brain tumor, SAR, Human head phantom

## 1. Introduction

Brain cancer is one of the serious public health problems worldwide because it affects the most vital organ of human body. For example, in the USA, 23,800 patients and 16,700 deaths are estimated due to brain cancer in 2017 [1]. Such a high death rate is caused by the invasive properties of tumors which turn brain cancer into a serious disease. But it is encouraging that the cure rate can be increased by reliably diagnosing it in the early stages because treatment at early stage is more efficient and effective compared with treatment done at the late stage of cancer. The common imaging modalities utilized to detect cancer are magnetic resonance imaging (MRI) scanning, x-ray screening, computed tomography (CT) scans, positron emission tomography (PET) and ultrasound imaging [2]. The possibility of microwave imaging technology for brain cancer detection is increased recently as it offers a safe, rapid, low-cost, noninvasive, and highly accurate system solution which involves nonionizing radiation [3].

Microwave imaging is an active wave-based non-invasive imaging method. Non-ionizing electromagnetic waves from microwave signals are able to penetrate human tissues without creating health hazards [4]. The contrast in the electrical properties between healthy and malignant tissues is the principal of operation of microwave imaging systems. Four large groups namely optimization-based microwave imaging, microwave tomography, confocal radar based imaging, and microwave holography can be considered as the branches of currently active microwave systems for tissue imaging [5]. Radar-based techniques are preferable since they only focus on detecting the tumor rather than the entire range of electrical properties [6]. Therefore, much easier signal processing such as less sophisticated delay and sum confocal microwave imaging algorithm is involved in radar-based microwave imaging.

Efficient design of transmitting/ receiving antenna is one of the prime aspects of any microwave based brain cancer detection system. So far in the literature, different types of antenna structure have been investigated as the radiating element in microwave imaging systems [7]-[9]. Microstrip patch antenna claims extra attention to be used in microwave brain imaging system as it acquires some unique properties such as compactness, easy construction, low cost, light weight, considerable gain and directivity [10]. However, conventional patch antennas need some modifications for reliable pulse transmission and collection of backscattered signals in microwave imaging systems. Amalgamation of electromagnetic band gap (EBG) structure on the antenna ground plane is found in the literature to be an effective way to enhance the performance of conventional microstrip patch antenna [11]. EBG

structures are any artificial periodic objects designed to prevent/ assist electromagnetic wave propagation in a given band of frequency. Due to their unique band gap features, EBG structures can be categorized as a special type of metamaterial. This unique property has been applied to design antenna systems with better gain and efficiency, reduced mutual coupling, lower side-lobes and back-lobe levels by suppressing surface wave modes [12], [13].

Assessment of specific absorption rate (SAR) induced inside human head is another important feature of any microwave brain imaging system. EM waves radiated from the transmitting antenna directly travel through the patients head and significant portion of the radiated power carrying by EM waves is absorbed by head tissues. These energy absorptions are not distributive in nature and may cause localized RF energy deposition in the form of nodes and damages DNA of living tissues which may trigger cell suicide or unregulated cell division resulting in the formation of a cancerous tumor [14]. Hence accurate SAR analysis which greatly depends on the exact head phantom model is a must one in imaging system to ensure the safety of patient under test. As the precise modeling of multi-layered human head consisting different complex tissues is cumbersome, various head phantom models have been investigated to mimic the practical scenario [15]-[17].

The goal of this study is twofold: 1) efficient and compact design of a microstrip patch antenna with EBG structures on the antenna ground plane, 2) detection of tumor inside human brain by radar based microwave brain imaging system. Patch antenna with circular EBG structure provides best performance and consequently it is applied in the brain tumor detection application. A six layer spherical human head phantom model having brain, CSF, dura, bone, fat, and skin as tissues and a tumor model inside head are designed. The dimensions and electrical properties of head and tumor models are chosen feasibly that reflect the actual ones. To get the imaging results, proposed antenna is simulated with head phantom model by CST MWS software. The S-parameter results obtained from different scanning modes involving head phantom with and without tumor model are applied in the microwave imaging algorithm to reconstruct tumor image. The SAR values for three different measuring techniques are compared with each other and with the established standard SAR limit so that safety of microwave brain tumor detection system is ensured. Thus, EBG based microstrip patch antenna is applied in brain tumor detection for the first time with all the necessary aspects of microwave brain imaging system being clearly analyzed.

## 2. System Model for Microwave Brain Imaging

Microwave brain imaging is based on the concept that a microwave signal is emitted from a transmitting antenna, which after being reflected from the target specimen is received by the receiving antenna. The received signal is stored and a suitable signal processing algorithm makes the image possible. The following Fig. 1 depicts the concept of our considered brain imaging system. In this system model, we specifically focus on the effective antenna modeling, human head phantom modeling, detection of tumor inside human brain by radar-based microwave image reconstruction algorithm, and determination of SAR values inside six layers human head model.

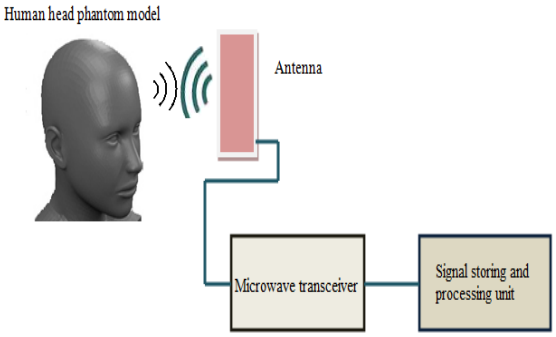


Fig. 1. Microwave brain imaging system model.

The head imaging architecture shown above primarily consists of a compact antenna to transmit and receive wideband signals, a microwave transceiver for signal generation and data acquisition and a personal computer for signal processing and image formation. A head imaging platform is designed

virtually in CST MWS software to evaluate the system's performance on detecting tumor using a realistic head phantom. The head phantom is scanned by changing the antenna position in different manner and the reflected signals are collected and converted from frequency domain to time domain. The resulting signals are then processed and used in confocal microwave image reconstruction algorithm to visualize the presence of tumor inside human head.

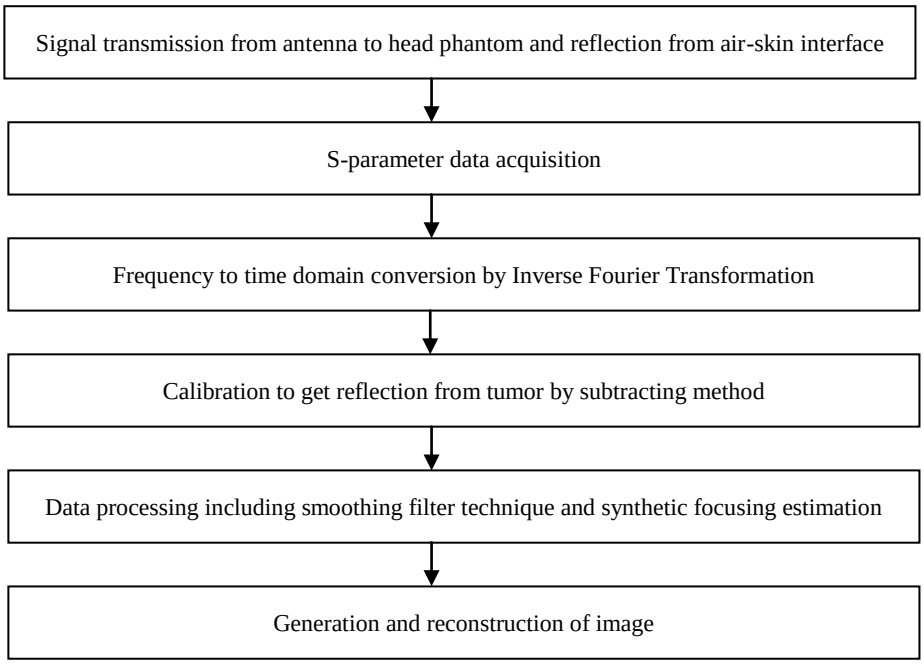


Fig. 2. Confocal microwave image reconstruction algorithm
for the considered brain imaging system model.

### 2.1. Patch antenna design

Herein we design a microstrip line feed rectangular patch antenna. The antenna resonant frequency is taken as 7.3 GHz. The following equations are used to design the rectangular patch [18].

Step-1: Patch width

$$w = \frac{v_0}{2f_r}\sqrt{\frac{2}{\varepsilon_r+1}} \tag{1}$$

Where, $v_0$ is velocity of light and $\varepsilon_r$ is dielectric constant of substrate.

Step-2: Effective Dielectric constant of the rectangular microstrip patch antenna

$$\varepsilon_{eff} = \frac{\varepsilon_r+1}{2} + \frac{\varepsilon_r-1}{2}\left(\frac{1}{\sqrt{1+\frac{12h}{w}}}\right) \tag{2}$$

Step-3: Patch Length

$$L = L_{eff} - 2\Delta L \tag{3}$$

$$L_{eff} = \frac{c}{2f_r\sqrt{\varepsilon_{eff}}} \tag{4}$$

Calculation of Length Extension,

$$\Delta L = 0.412h\frac{(\varepsilon_{eff}+0.3)(\frac{w}{h}+0.264)}{(\varepsilon_{eff}-0.258)(\frac{w}{h}+0.8)} \tag{5}$$

Step-4: Inset Feed

$$50 = R_{in}\left(\cos\left(\frac{\pi}{L}y_0\right)\right)^2 \tag{6}$$

Where, $R_{in}$ is the input impendence at the leading radiating edge of the patch and 50 Ω is the desired impendence. The complete design of the rectangular patch antenna with all required dimensions is shown in Fig. 3. Rogers R03003 is chosen as antenna substrate due to its flexibility for high frequency application compared to FR4 substrate. The choice of appropriate substrate thickness plays an important role in the patch antenna design. The antenna efficiency and bandwidth can be increased by increasing the substrate height, but at the cost of introducing surface waves which extract power from the total available for direct radiation [18].

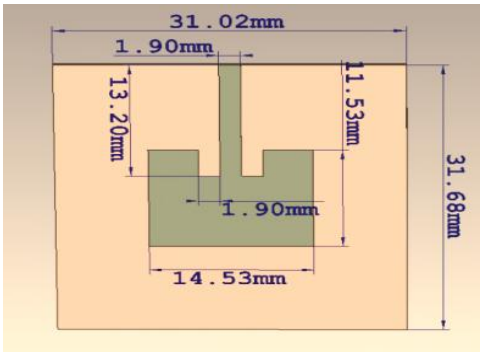


Fig. 3. Schematic diagram of patch antenna without EBG structure.

## 2.2. EBG structure design

The wavelength of the microwave signal radiated by the proposed antenna is used to design the EBG structures. The effect of EBG structure is found to be the reduction of patch length, substrate length, inset gap and an increase in substrate height. Following are the equations required to design the proposed EBG structures.

$$L = 0.10\lambda \tag{7}$$

$$D = 0.02\lambda \tag{8}$$

$$r = 0.10\lambda \tag{9}$$

Where, L is the length and r is the radius of the rectangular and circular EBG structures respectively and D is the distance between two shapes in any case as evident from Fig. 4. Nicholson-Ross-Weir (NRW) technique is used as a conversion approach in designing the proposed EBGs. Both permeability and permittivity is obtained from S-parameter using this approach [19].

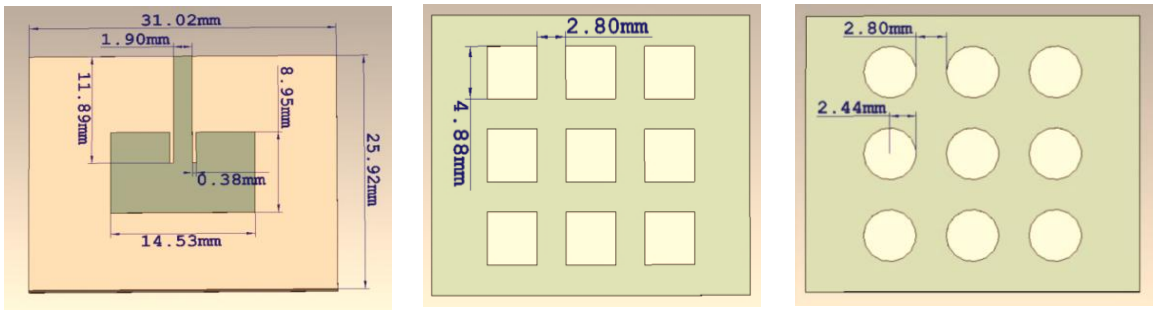


(a) (b) (c)

Fig. 4. Schematic diagram of (a) patch antenna with EBG, (b) geometry of circular EBG,

(c) geometry of rectangular EBG.

The initial dimension parameters of the patch antenna are obtained from the established equations. However, after incorporating the EBG structure on the antenna ground plane, the dimension parameters are slightly optimized to obtain enhanced performance. The effect of optimization is found to be the reduction in patch length, substrate length, and inset gap. Hence incorporation of the EBG structure makes the antenna more compact. Also the surface wave introduced in the antenna is sufficiently

reduced due to the incorporation of EBG structure on the antenna ground plane. All the dimension parameters to design patch antenna without EBG and with circular EBG are given in the following table.

Table I

Rectangular microstrip patch antenna specifications

| **Design parameters** | **Dimensions without EBG (mm)** | **Optimized dimensions with circular EBG shape (mm)** |
|---|---|---|
| Patch Width, W | 14.53 | 14.53 |
| Patch Length, L | 11.53 | 8.95 |
| Inset Feed, $y_0$ | 3.125 | 3.41 |
| Inset Gap, g | 1.901 | 0.38 |
| Feed Length, $L_f$ | 13.202 | 11.895 |
| Feed Width, $W_f$ | 1.901 | 1.9010 |
| Substrate Width, $W_S$ | 31.02 | 31.0170 |
| Substrate Length, $L_S$ | 31.68 | 25.92 |
| Substrate Thickness, h | 0.75 | 1.03 |
| Resonant Frequency, $f_c$ | 7.3GHz | |

### 2.3. Human head and tumor modeling

The dielectric properties, i.e. permittivity and conductivity of human body tissues vary with frequency, geometry, size of tissue, water contents and age. Since the SAR measurements and EM field evaluation inside the human body are quite difficult, phantom models of different shapes have been designed in the literature to conduct the desired EM measurement for any imaging system. A schematic representation of the designed spherical head phantom is shown in the following Fig. 5.

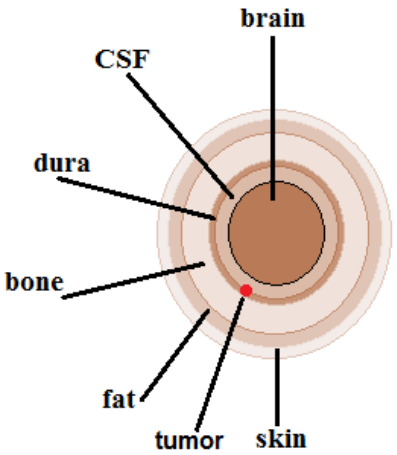


Fig. 5. Six layer human head phantom with tumor model

A human brain model with tumor inside it, as shown in Fig. 5, is used in the simulation. The tumor is placed in between CSF and dura close to the bone. The radiated signals from the antenna start penetrating the outer tissue layer and gradually move toward the inner layer. However, attenuation of RF energy occurs very quickly due to backscatter from each tissue layer. Therefore, the tumor is placed close to the bone so that in can be easily detected from the simulation results. In contrast, detection of

heavily buried tumor inside multi-layer human brain becomes difficult as the reflected signal from tumor in this case could be too weak. The dimension and dielectric properties of all head tissues and tumor model are tabulated below.

Table II

Dimensions and electrical properties of head tissues and tumor model

| **Tissue** | **Radius (mm)** | **Permittivity, ($\epsilon_r$)** | **Conductivity, σ (S/m)** |
|---|---|---|---|
| Brain | 81 | 43.22 | 1.29 |
| CSF | 83 | 70.1 | 2.3 |
| Dura | 83.5 | 46 | 0.9 |
| Bone | 87.6 | 5.6 | 0.03 |
| Fat | 89 | 5.54 | 0.04 |
| Skin | 90 | 45 | 0.73 |
| Tumor | 5 | 55 | 7 |

To simplify the simulation study, tumor and a six layer specific anthropomorphic mennequin (SAM) phantom head is modeled considering the above realistic dielectric tissue properties in the frequency band of interest. Though anatomically non-realistic, as is often the case found in literature, a spherical head phantom can be considered as a feasible one for microwave imaging and SAR evaluation in the simulation environment. Patch antenna with circular EBG structure located at 10 mm distance from the head model for suitable penetration of microwave signal inside the tissue layers is illustrated in the following Fig. 6.

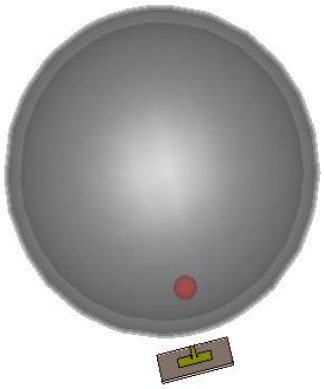

Fig. 6. Patch antenna with human head and tumor modeling in CST.

## 3. Results and Discussions

Finite element method (FEM) based CST MWS software is used to simulate the proposed antenna and to evaluate the SAR values induced inside head tissues. The antenna performance parameters to be considered are the return loss, gain, and bandwidth. S-parameter signals obtained from simulation in different scanning modes are analyzed by MATLAB software to reconstruct tumor image. Biocompatibility analysis of the phantom head model is carried out by measuring the 1g average, 10g average, and point SAR. The averaging volume for maximum SAR is also plotted to clearly locate the maximum SAR position.

### 3.1. Antenna return loss, bandwidth, and gain

The S-parameters of any antenna must be at least -10 dB to ensure the minimum reflection from antenna to the source. Particularly in a brain imaging application, the return loss must be as lowest as

possible so that sufficient amount of power can be radiated to the target specimen. In microwave imaging, the resolution of the reconstructed image mostly depends on the magnitude of the scattered signal from the target which in turn depends on the amount of total radiated power from the transmitting antenna. Hence to ensure the good image quality, the return loss of the proposed antenna should be minimized. Fig. 7 (a) represents the return loss of the designed patch antenna without and with rectangular EBG structure. It's evident from the figure that rectangular EBG structure on the antenna ground plane improves the return loss from -18.402 dB to -40.146 dB. Fig. 7 (b) reveals a further enhancement in the reflection coefficient to -49.289 dB which is made possible by the incorporation of circular EBG structure on antenna ground plane. Bandwidth is another antenna performance parameter which needs to be taken into account for an appropriate imaging system. Ultra wideband antenna is always preferable in microwave brain imaging for a reliable system operation. In case of bandwidth, patch antenna without the EBG structure provides 156.20 MHz, with rectangular EBG structure provides 275.50 MHz, and with circular EBG structure provides 291.60 MHz.

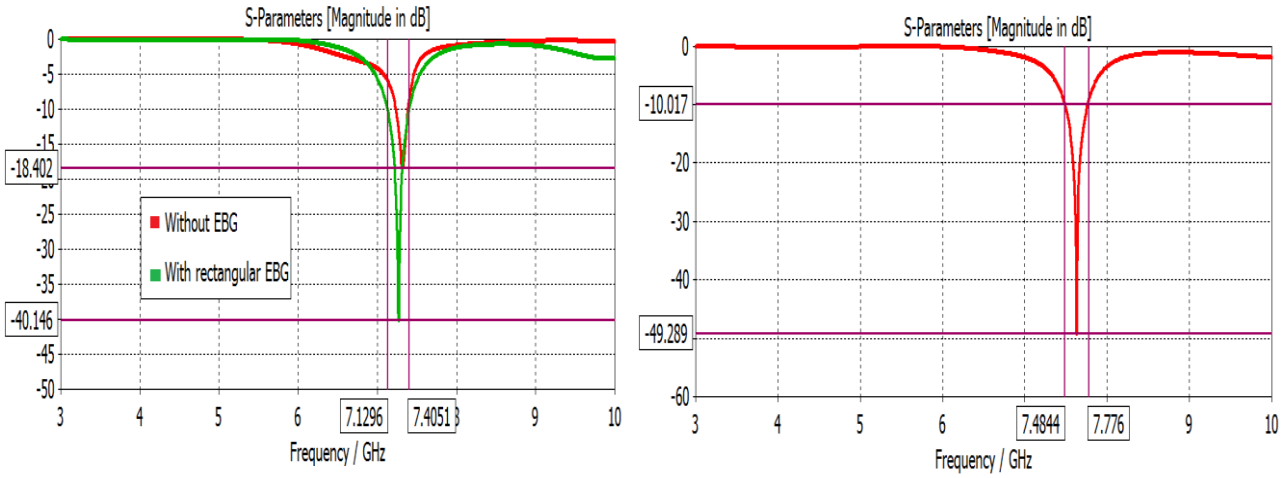


Fig. 7. (a) Return loss of the patch antenna without EBG and with rectangular EBG, (b) antenna return loss with circular EBG.

Hence the introduction of circular EBG structure perfectly improves the antenna performance in terms of return loss and bandwidth. The polar plot of directivity and 3-D plot of gain of the patch antenna with rectangular and circular EBG structure are shown in Fig. 8. Information obtained from Fig. 8 (a) indicates that the proposed patch antenna with circular EBG structure provides a directivity of 6.77 dBi in the direction of φ =31°. The values of 3 dB beamwidth and side lobe level found from the same figure are 92.6° and -8.9 dB respectively.

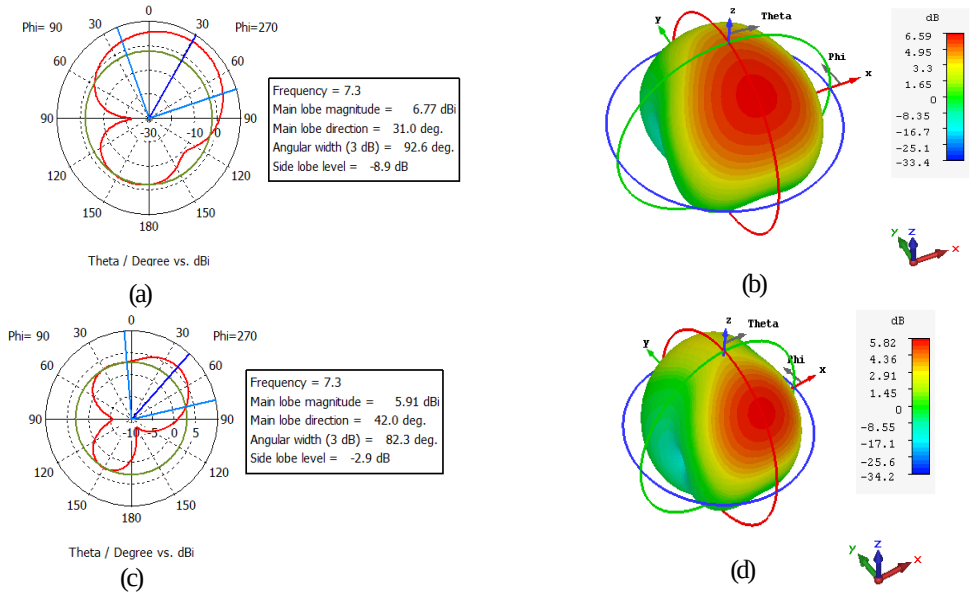


Fig. 8. (a) Polar plot of directivity, (b) 3-D plot of gain of patch antenna with circular EBG, (c) polar plot of directivity, and (d) 3-D plot of gain of patch antenna with rectangular EBG.

The increased beamwidth will ensure the resolution capabilities of the antenna while reduced side lobe level is an indication of greater radiation intensity in the main lobe. Fig. 8 (c) shows the polar plot of directivity of microstrip patch antenna with rectangular EBG structure on the ground plane. The lower value of directivity, i.e. 5.91 dBi for rectangular EBG as compared with 6.77 dBi for circular EBG makes patch antenna with rectangular EBG less compatible for brain imaging application. Gain is another useful measure to describe the performance of an antenna as it takes into account the efficiency as well as directional capabilities of the antenna. The simulated gain of the proposed antenna with circular and rectangular EBG structure as shown in Fig. 8 (b) and (d) are 6.59 dB and 5.82 dB respectively. The higher gain offered for circular EBG is a consequence of strong surface wave reduction which indicates a greater potentiality of patch antenna with circular EBG to be applied in microwave brain tumor detection.

Table III

Performance comparison of the proposed antenna with other existing antennas

| **Parameter** | **Proposed antenna** | **[20]** | **[12]** | **[21]** |
|---|---|---|---|---|
| Return Loss (dB) | -49.289 | -18 | -22 | -17.50 |
| Gain (dB) | 6.59 | - | - | 5.01 |
| Bandwidth (MHz) | 291.60 | 190 | - | - |
| Directivity (dBi) | 6.77 | 2.5 | 2.2 | - |

Finally, a comparison between the performance parameters of the proposed antenna and similar other existing antennas is given in Table III. Similar other antennas mean those designed incorporating any metamaterial structure. It's obvious from the comparison that the proposed microstrip patch antenna with circular EBG structure provides enhanced performances which can be a reliable candidate for microwave brain imaging.

### 3.2 Brain tumor detection

A sequence of task is done as depicted in the algorithm in Fig. 2 to detect the tumor inside head phantom using a mono-static radar-based confocal microwave image reconstruction system.

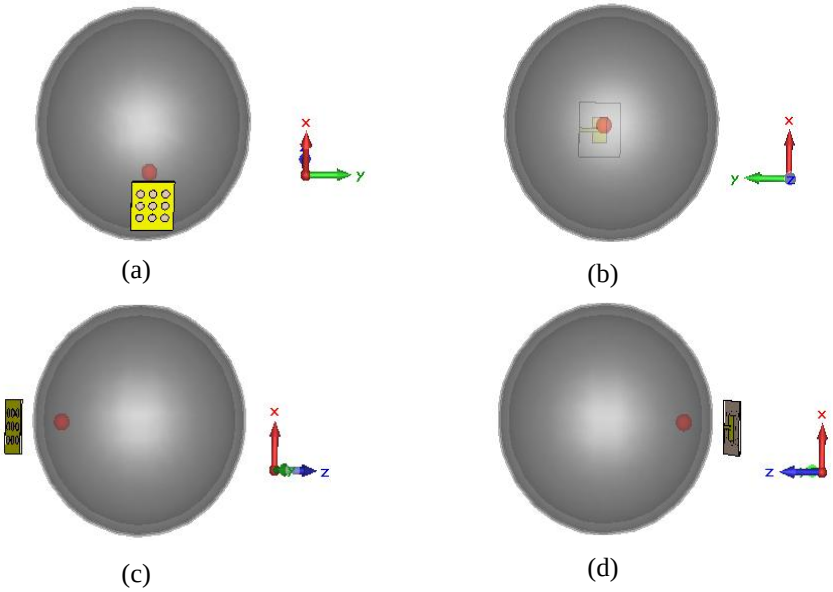


Fig. 9. Position of antenna for scanning the phantom in (a) x-y plane, (b) reverse x-y plane, (c) x-z plane, (d) reverse x-z plane.

Mono-static radar-based technique adopted in this work is based on the concept where a single antenna scans the head phantom by mechanically rotating around it. However, in CST simulation environment, mechanical rotation is accomplished by moving the antenna to all the possible locations around the phantom and simulating the system for each antenna location. Fig. 9 illustrates the antenna positions around the head phantom in different scanning mode. Fig. 9 (a) and (c) show the scanning in x-y and x-z plane. To get a clearer visualization of the 3-D system in 2-D plane, Fig. 9 (b) and (d) provide scanning performance in reverse x-y and reverse x-z plane. In all these scanning modes, multiple reflections from different head tissue layers and tumor response, and noise are contained in the collected scattering signals. As the microwave signal reaches tumor after penetrating some complex tissue layers, sufficient signal attenuation occurs which make tumor response quite weak resulting in an easy drowning out in the noise. Therefore, signal processing is a must one to remove all the unwanted signals which results in a high resolution image with low noise level for reliable diagnosis. A reference transient scattering signal using a head phantom without tumor being presence is needed to remove all unwanted parts of signal. By subtracting the reference signal from originally received signal, tumor response can be extracted. To obtain the reference and original signals, proposed antenna is simulated using head phantom with and without tumor. Reflection coefficient

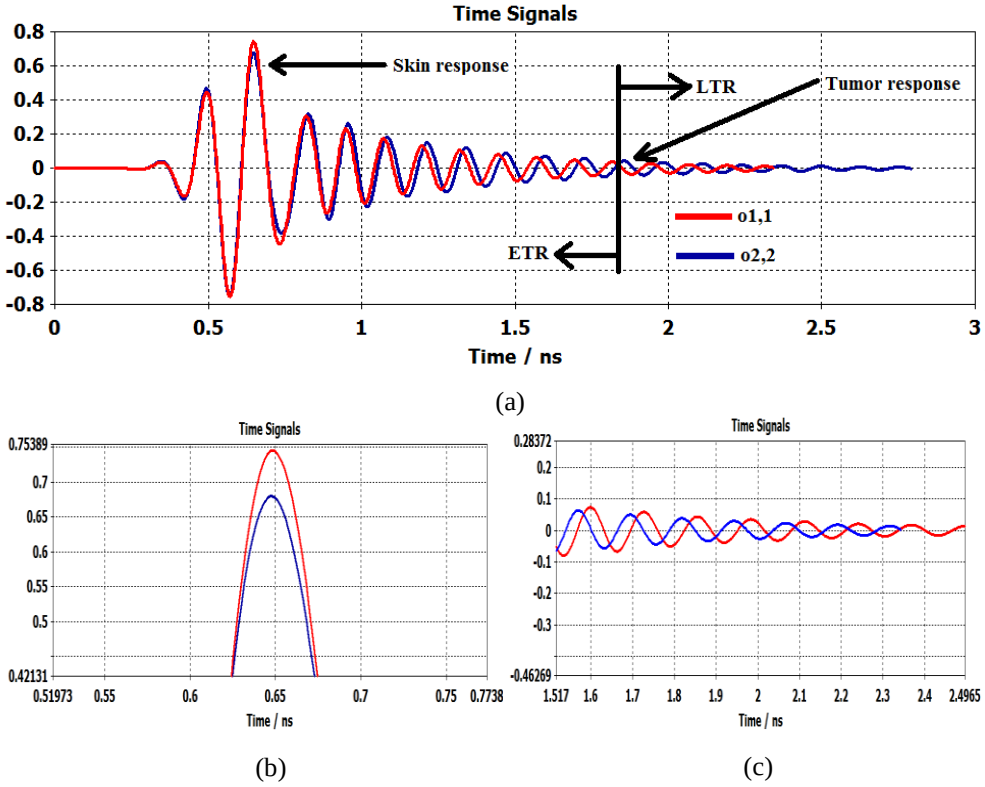


Fig. 10. (a) Reflected transient signal by simulating antenna using head phantom with and without tumor, (b) enlarged skin response, (c) enlarged tumor response

for original and reference signals are shown in Fig. 10 (a). o1,1 and o2,2 represent the reflected energy from head phantom with and without tumor respectively. ETR and LTR stand for early time response and late time response respectively. When a cancerous human head is illuminated by an incident EM wave, skin and other head tissue layer contained in the scattering wave involves the optical region, which means that these reflections contribute to the ETR. The tumor reflection is involved with the resonance region and contributes to the LTR. Hence, skin and tumor responses can be extracted by investigating the turn on time of LTR which is defined as twice the time taken by incident EM wave to pass through the surface of the object [22]. Fig. 10 (b) shows that the energy reflected from skin layer of head phantom with tumor is greater than that without tumor. The strong reflection from the high permittivity tumor tissue is the reason behind this result. Enlarged portion of tumor response is illustrated in Fig. 10 (c) which shows that reflected transient signal for head phantom without tumor becomes steady state quicker than that with tumor.

From the above discussion it's clear that the reflected energy depends on the presence of tumor which in turn depends on antenna position. This basic principle is used to generate microwave images by moving the antenna to different locations surrounding the spherical human head phantom, with scattering signals recorded at each stop location. The images are created by using the intensities of the scattering signals at each scan position. The resulting microwave image of tumor inside multi-layer human head phantom is

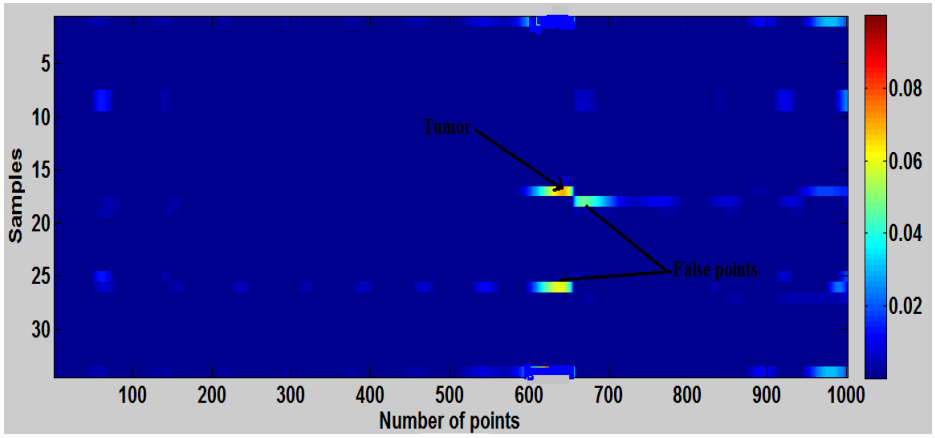


(a)

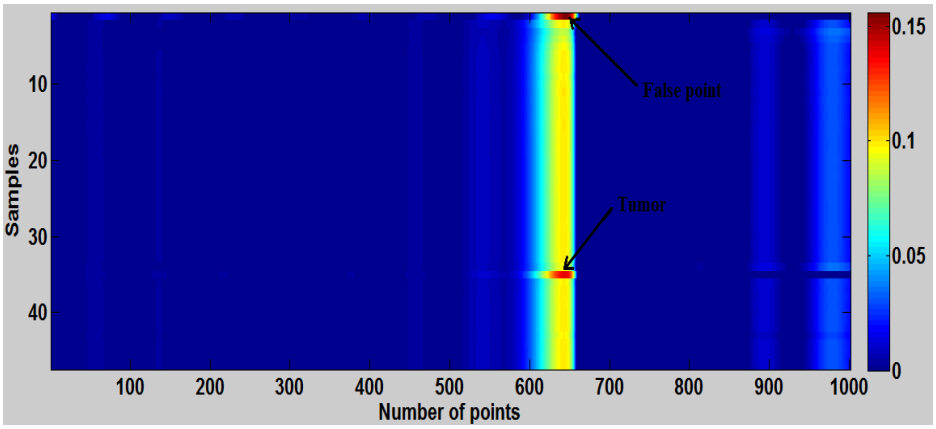


(b)

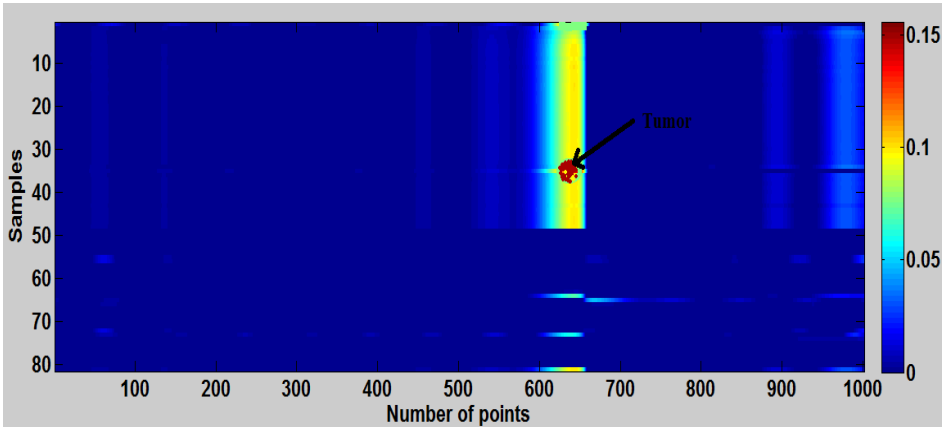


(c)

Fig. 11. Reconstructed microwave image of tumor by scanning head phantom in (a) x-y plane, (b) x-z plane, and (c) x-y and x-z plane.

shown in Fig. 11. Presence of tumor with two false points can be observed in Fig. 11 (a) where scanning is performed in x-y plane. Due to reflections from different tissue layers in a cylindrical scanning mode in x-y plane, presence of two false points and a non-spherical shaped tumor are evident from Fig. 11 (a). When the same rotational scanning is done in x-z plane, resolution of image is increased and number of false point is decreased. This improvement is accomplished because the pulse from antenna in this case is transmitted to a more exact z direction. However, the reconstructed image still contains some noise in the form of false point due to the inability of radiation pattern of the antenna to cover the whole round phantom. To overcome these difficulties, a combined rotational scanning is carried out where the data from rotational scanning in x-y and x-z plane are combined together. The reconstructed image for combined scanning mode is shown in Fig. 11 (c) where the resolution and shape of tumor are fairly good with minimal possibility of false diagnosis. Therefore microwave imaging via combined rotational scanning of a multi-layer human head phantom can reliably detect the presence of tumor inside the human head.

### 3.3 Evaluation of specific absorption rate (SAR)

The safety regulation of microwave based brain imaging system must be maintained by proper assessment of SAR as a brief exposure to radiation may cause severe health hazard. SAR is a measure of the deposition of electromagnetic energy over time into human body tissue. The units are generally watts per kilogram of body mass. In mathematical form, it is defined as [23]:

$$\mathrm{SAR} = \frac{\sigma}{\rho}|\mathrm{E}|^2 = \frac{\mathrm{J}^2}{\rho\sigma}\ [\mathrm{W/kg}] \tag{10}$$

Where, $E$ is the rms value of the electric field strength in the tissue [V/m], $J$ is the current density [A/m], $\sigma$ is the conductivity of the head tissue [S/m], and $\rho$ is the density of head tissues [kg/m$^3$].

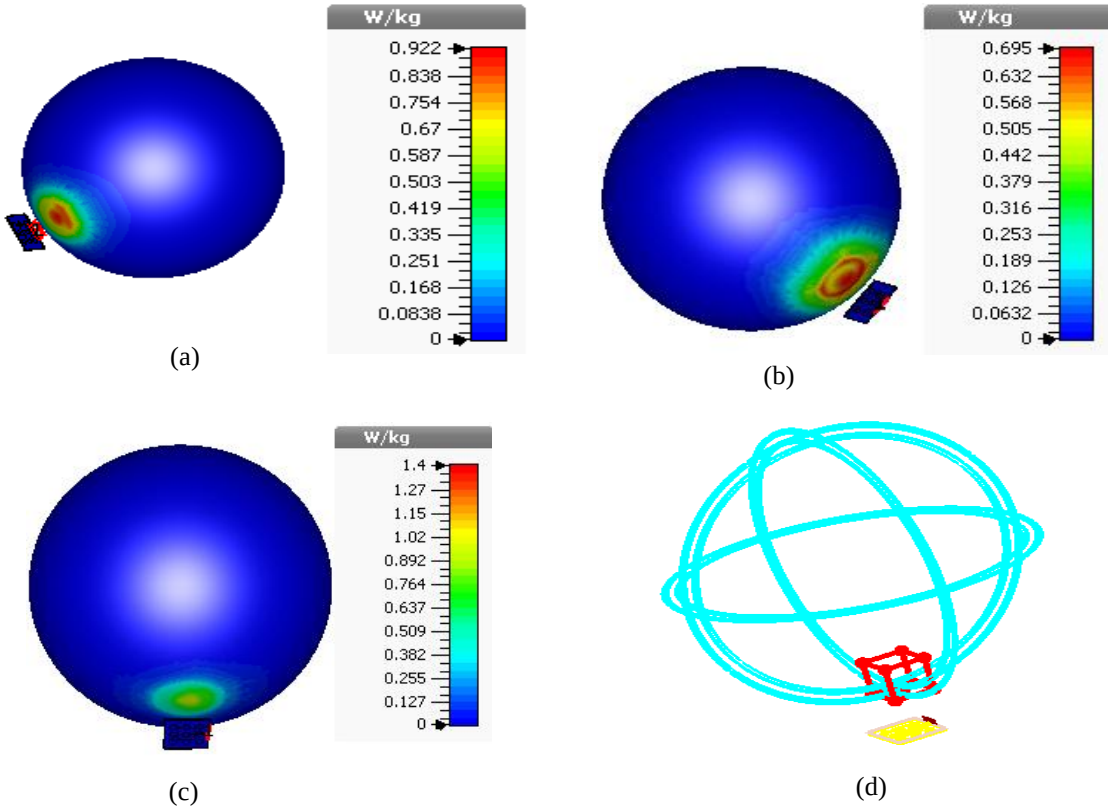


Fig. 12. (a) 1g average SAR, (b) 10g average SAR, (c) point SAR, and (d) 10g averaging volume for maximum SAR value for patch antenna with circular EBG structure.

Different techniques are available to assess the SAR value of human body tissue when exposed to EM radiation. The antenna type, operating frequency, and distance between the antenna and body tissue are the key parameters that affect the determination of SAR. Depending on national reporting, testing requirement, and the network band, the international SAR limit may vary. Averaged on 1g of tissue, the SAR limit set by

US is 1.6 W/kg while in EU, the limit is 2.0 W/kg, averaged on 10g of tissue [24]. The 3-D plot obtained by numerical method based EM simulation of SAR distribution in the six layered head phantom model is depicted in Fig. 12. For mass averaged SAR, the power loss density is integrated over a cube with a defined mass, typically 1g or 10g. The integral power loss is then divided by the cube's mass. Thus the 1g average and 10g average SAR values are evaluated which are evident from Fig. 12(a) and 12(b) respectively. It's also obvious from Fig. 12(a) and 12(b) that the 3-D maximum SAR values are 0.922 W/kg and 0.695 W/kg, which are less than maximum standard limit as 1.6 W/kg and 2.0 W/kg, averaged on 1g and 10g of tissue respectively. Fig. 12(c) represents the point SAR which is local SAR without mass or volume averaging. In all cases, the reference stimulated power is taken as 0.5 W. In Fig. 12(d), 10g averaging maximum SAR cube is visualized. It's clear from Fig. 8 that the SAR value is higher near the antenna and then rapidly decreases to zero after a short distance. Hence, this microwave brain imaging system employing circular EBG based microstrip patch antenna maintains the safety regulation.

## 4. Conclusion

A brain imaging system working in microwave frequency range for human brain tumor detection is envisaged. An efficient microstrip patch antenna is devised whose performance is improved by slotting circular EBG structure on the antenna ground plane. The unique band gap feature of circular EBG configuration boosts antenna performance parameters namely return loss, gain, bandwidth, and directivity by considerable suppression of surface wave introduced on antenna substrate. The optimized and enhanced patch antenna based on circular EBG is applied in the considered imaging application. The antenna is used to scan a spherical six-layer human head phantom model. The S-parameter data obtained from a combined rotational scanning mode performed in x-y and x-z plane, is utilized in a confocal microwave imaging algorithm to detect tumor inside the human brain. Finally, assessment of specific absorption rate (SAR) induced inside the human head phantom is carefully done. The overall results obtained confirm that the studied brain imaging system can successfully diagnose brain tumor at an early stage while maintaining safety regulation of the patient under test.

### Conflict of Interest

The authors declare that there is no conflict of interest regarding the publication of this paper.

## References


[1] R. L. Siegel, K. D. Miller, and A. Jemal, "Cancer statistics, 2017," *CA Cancer J Clin*, vol. 00, no. 00, pp. 1-24, 2017.

[2] B, J. Mohammed, A. M. Abbosh, S. Mustafa, and D. Ireland, "Microwave system for head imaging," *IEEE Trans. Instrum. Meas.*, vol. 63, pp. 117-123, Jan. 2014.

[3] M. Ostadrahimi, P. Mojabi, S. Noghanian, L. Shafai, S. Pistorius, and J. LoVetri, "A novel microwave tomography system based on the scattering probe technique," *IEEE Trans. Instrum. Meas.*, vol. 61, no. 2, pp. 379–390, Feb. 2012.

[4] F. S. G. B. Barnes, "Handbook of biological effects of electromagnetic fields," *CRC/ Taylor & Francis,Boca Raton*, 2007.

[5] N. K. Nikolova, "Microwave imaging for breast cancer," *IEEE Micro. Magzn.* vol. 12, no. 7, pp. 78-94, 2011.

[6] A. E. Souvorov, A. E. Bulyshev, S. Y. Semenov, R. H. Svenson, and G. P. Tatsis, "Two-dimensional computer analysis of a microwave flat antenna array for breast cancer tomography," *IEEE Trans. Micro. Theory Tech.* vol. 48, no. 8, pp. 1413-1415, 2000.

[7] M. T. Islam *et al.,* "A negative index metamaterial-inspired UWB antenna with an integration of complementary SRR and CLS unit cells for microwave imaging sensor applications," *Sensors*, vol. 15, pp. 11601-11627, May. 2015.

[8] A. T. Mobashsher and A. Abbosh, "CPW-fed low profile directional antenna operating in low microwave band for wideband medical diagnostic system," *Electron. Lett.*, vol. 50, pp. 246-248, Feb. 2014.

[9] M. Klemm, I. J. Craddock, A. Preece, J. Leendertz and R. Benjamin, "Evaluation of a hemi-spherical wideband antenna array for breast cancer imaging," *Radio Sci.*, vol. 43, pp. 1-15, 2008.

[10] I. Singh *et al.,* "Microstrip patch antenna and its applications: a survey," *Int. J. Comput. Applicat. Tech.*, vol. 2 (5), pp. 1595-1599, 2011.

[11] L. Zhang, "Numerical characterization of electromagnetic band-gap materials in printed antennas and arrays," *Ph. D. Dissertation, Electrical Engineering Dept., University of California, Los Angeles*, 2000.

[12] J. Liang, and H. Y. D. Yang, "Microstrip patch antennas on tunable electromagnetic band-gap substrates," *IEEE Trans. Antennas Propag.*, vol. 57, pp. 1612-1617, Jun. 2009.

[13] M. F. Abedin, M. Z. Azad, and M. Ali, "Wideband smaller unit-cell planar EBG structures and their application," *IEEE Trans. Antennas Propag.*, vol. 56, pp. 903-908, Mar. 2008.

[14] M. Mashevich, "Exposure of human peripheral blood lymphocytes to electromagnetic fields associated with cellular phones leads to chromosomal instability," *Bioelectromagnetics (USA)*, vol. 24, no. 82, 2003.

[15] M. R. I. Faruque *et al.*, "Effect of human head shapes for mobile phone exposure on electromagnetic absorption," *InformacijeMIDEM*, vol. 40, pp. 232-237, 2010.

[16] M. S. M. Said, N. Seman, and H. Jaafar, "Characterization of human head phantom based on its dielectric properties for wideband microwave imaging application," *J. Teknologi (Sci. Eng.)*, vol. 73, no. 6, pp. 43-49, Apr. 2015.

[17] S. Mustafa, A. M. Abbosh and P. T. Nguyen, "Modeling human head tissues using fourth-order Debye model in convolution-based three dimensional finite-difference time-domain," *IEEE Trans. Antennas Propag.*, vol. 62, pp. 1354-1361, Mar. 2014.

[18] C. A. Balanis. "Antenna theory analysis and design," *A John Wiley & Sons, Inc.*, 3rd edition, 2005.

[19] C. Y. Kuek, "Measurement of dielectric material properties," *Rohde & Schwarz Application Note,RAC0607-0019*, 2006.

[20] A. S. Bhadouria, and M. Kumar, "Microstrip patch antenna for radiolocation using DGS with improved gain and bandwidth," *IEEE Int. Conf. Advances Eng. Tech. Research*, pp. 1-5, Aug. 2014.

[21] S. E. Mendhe, and Y. P. Kosta, "Gain enhancement and broadband using helical resonating metamaterial superstrate in stacked microstrip patch antenna," *Microw. Optic. Tech. Lett.*, vol. 56, no. 9, pp. 1978-1982, Sep. 2014.

[22] S. K. Hong, W. S. Wall, T. D. Andreadis, and W. A. Davis, "Practical implications of poles series convergence and the early-time in transient backscatter," *NRL Memorandum Report*, NRL/MR/5740--12-9411, Apr. 2012.

[23] M. K. Hosain *et al.*, "Development of a compact rectenna for wireless powering of a head-mountable deep brain stimulation device," *IEEE J. Transl. Eng. Heal. Medic.*,vol. 2, Jan. 2014.

[24] Antenna-Theory.com,"Specific Absorption Rate (SAR)," 2014. [online]. Available: http://www.antennatheory.com/ definitions/ sar.php.